Nck adaptor proteins control the organization of neuronal circuits important for walking

James P. Fawcett*†‡, John Georgiou*, Julie Ruston*, Friedhelm Bladt*§, Andrew Sherman*¶, Neil Warner*¶, Bechara J. Saab*¶, Rizaldy Scott*, John C. Roder*¶, and Tony Pawson*¶‖

*Samuel Lunenfeld Research Institute, Mount Sinai Hospital, 600 University Avenue, Toronto, ON, Canada M5G 1X5; ¶Department of Medical Genetics and Microbiology, University of Toronto, 1 Kings College Circle, Toronto, ON, Canada M5S 1A8; and †Departments of Pharmacology and Surgery, Dalhousie University, 5850 College Street, Halifax, NS, Canada B3H 1X5

Contributed by Tony Pawson, October 31, 2007 (sent for review August 28, 2007)

The intracellular signaling targets used by mammalian axon guidance receptors to organize the nervous system *in vivo* are unclear. The Nck1 and Nck2 SH2/SH3 adaptors (collectively Nck) can couple phosphotyrosine (pTyr) signals to reorganization of the actin cytoskeleton and are therefore candidates for linking guidance cues to the regulatory machinery of the cytoskeleton. We find that selective inactivation of Nck in the murine nervous system causes a hopping gait and a defect in the spinal central pattern generator, which is characterized by synchronous firing of bilateral ventral motor neurons. Nck-deficient mice also show abnormal projections of corticospinal tract axons and defective development of the posterior tract of the anterior commissure. These phenotypes are consistent with a role for Nck in signaling initiated by different classes of guidance receptors, including the EphA4 receptor tyrosine kinase. Our data indicate that Nck adaptors couple pTyr guidance signals to cytoskeletal events required for the ipsilateral projections of spinal cord neurons and thus for normal limb movement.

axon guidance | locomotion | SH2/SH3 adaptors | EphA4

Axon guidance depends on the integration of signals from activated receptors and adhesion molecules to the growth-cone cytoskeleton. Our understanding of the mechanisms involved in transducing signals from these receptors to the actin cytoskeleton to influence growth-cone turning remain incomplete. One important family of proteins involved in mediating phosphotyrosine-based signals are the Nck adaptor proteins Nck1 and Nck2. Nck proteins contain a C-terminal SH2 domain that binds preferentially to pY-D-X-V motifs (1) and three N-terminal SH3 domains that associate with proteins implicated in the regulation of the actin cytoskeleton, including N-WASP and the Pak serine/threonine kinases (2). Nck adaptors are therefore candidate targets for cell-surface receptors that modify the actin cytoskeleton in processes such as axon guidance. Consistent with this possibility, a number of guidance receptors can associate with Nck, including the B-type Eph receptors (3, 4) and their transmembrane ephrin ligands (5), Robo (6) and the netrin receptor DCC (7), as well as cytoplasmic docking proteins such as Dok1 (3), disabled-1 (8), and p130^{cas} (9). Furthermore the *Drosophila* orthologue of Nck, dreadlocks (Dock), is important for photoreceptor cell (R cell) axon guidance (10), in conjunction with Pak (11).

To date, analysis of the role of mammalian Nck proteins in neuronal development has been limited by the observation that mice homozygous for null alleles of either *Nck1* or *Nck2* alone appear normal, whereas mice lacking both Nck1 and Nck2 die at embryonic day 9.5 (12). Here we report that selective inactivation of Nck in the developing nervous system results in animals that display locomotor defects. Consistent with this phenotypic abnormality, we find defects in the response of corticospinal tract neurons to midline cues in these mice. Furthermore, we identify alterations in the local rhythmic pattern of flexor and extensor muscles by using isolated spinal cord preparations, and we identify guidance defects of ventral spinal interneurons in Nck-deficient animals. These phenotypes are similar to those exhibited by EphA4 null mice, suggesting that Nck is an important downstream effector of EphA4 in controlling axon guidance.

Results and Discussion

Mice Lacking Nck Protein in the Developing Nervous System Exhibit Locomotor Defects. Mice have two closely related *Nck* genes (*Nck1* and *Nck2*) that have overlapping functions; animals lacking either gene alone are viable, whereas double mutants die at embryonic day 9.5 (12). To explore the importance of Nck in the mammalian nervous system, we used a conditional allele of the *Nck2* gene (*Nck2^{flx}*), in which loxP sites flank the first coding exon (1) [Fig. 1 *a* and *b* and supporting information (SI) Fig. 5*a*]. We confirmed the ability of Cre recombinase to inactivate expression of the *Nck2^{flx}* allele in mouse embryo fibroblasts (SI Fig. 5*b*). We then generated mice that were homozygous for both an *Nck1*-null allele and the *Nck2^{flx}* allele and that carried a *Nestin-Cre* transgene to selectively inactivate *Nck2* in neuronal and glial cell precursors (13) (*Nck1$^{-/-}$;Nck2$^{flx/flx}$;Nestin-Cre*, subsequently termed "Nck-deficient"). These mice showed a strong reduction of detectable Nck protein levels in the brain (Fig. 1*c*, top gel), but not in nonneuronal tissues such as the liver (Fig. 1*c*, bottom gel). Similarly, dissociated embryonic cortical neurons showed a dose-dependent loss of Nck protein expression (Fig. 1*d*). These animals were born at the expected Mendelian frequency (Fig. 1*e*) and were viable and fertile. However they exhibited a hopping gait that was maintained to adulthood (Fig. 1 *f* and *g*).

Corticospinal Tract Defects in Nck-Deficient Mice. The inability of adult Nck-deficient mice to alternate their limb movements suggested the possibility of defects in the corticospinal tract (CST), a major axon tract important in regulating gait (14). Cross-sections through both the thoracic and lumbar regions of the spinal cord of adult Nck-deficient animals revealed a shallow dorsal funiculus (DF) ($n = 8$) compared with control mice ($n = 5$) (Fig. 1 *h–k*), consistent with defects in the CST. We therefore performed anterograde axon tracing experi-

Author contributions: J.G. and J.R. contributed equally to this work; J.P.F. and T.P. designed research; J.P.F., J.G., J.R., F.B., A.S., N.W., B.J.S., and R.S. performed research; F.B. contributed new reagents/analytic tools; J.P.F., J.G., J.R., J.C.R., and T.P. analyzed data; and J.P.F., J.G., and T.P. wrote the paper.

The authors declare no conflict of interest.

Freely available online through the PNAS open access option.

‡To whom correspondence may be sent at the † address. E-mail: jim.fawcett@dal.ca.

§Present address: Experimental Therapeutics and Translational Research, Oncology Sanofi Aventis 13, Quai Jules Guesde, 94403 Vitry Sur Seine, France.

‖To whom correspondence may be sent at the * address. E-mail: pawson@mshri.on.ca.

This article contains supporting information online at www.pnas.org/cgi/content/full/0710316105/DC1.

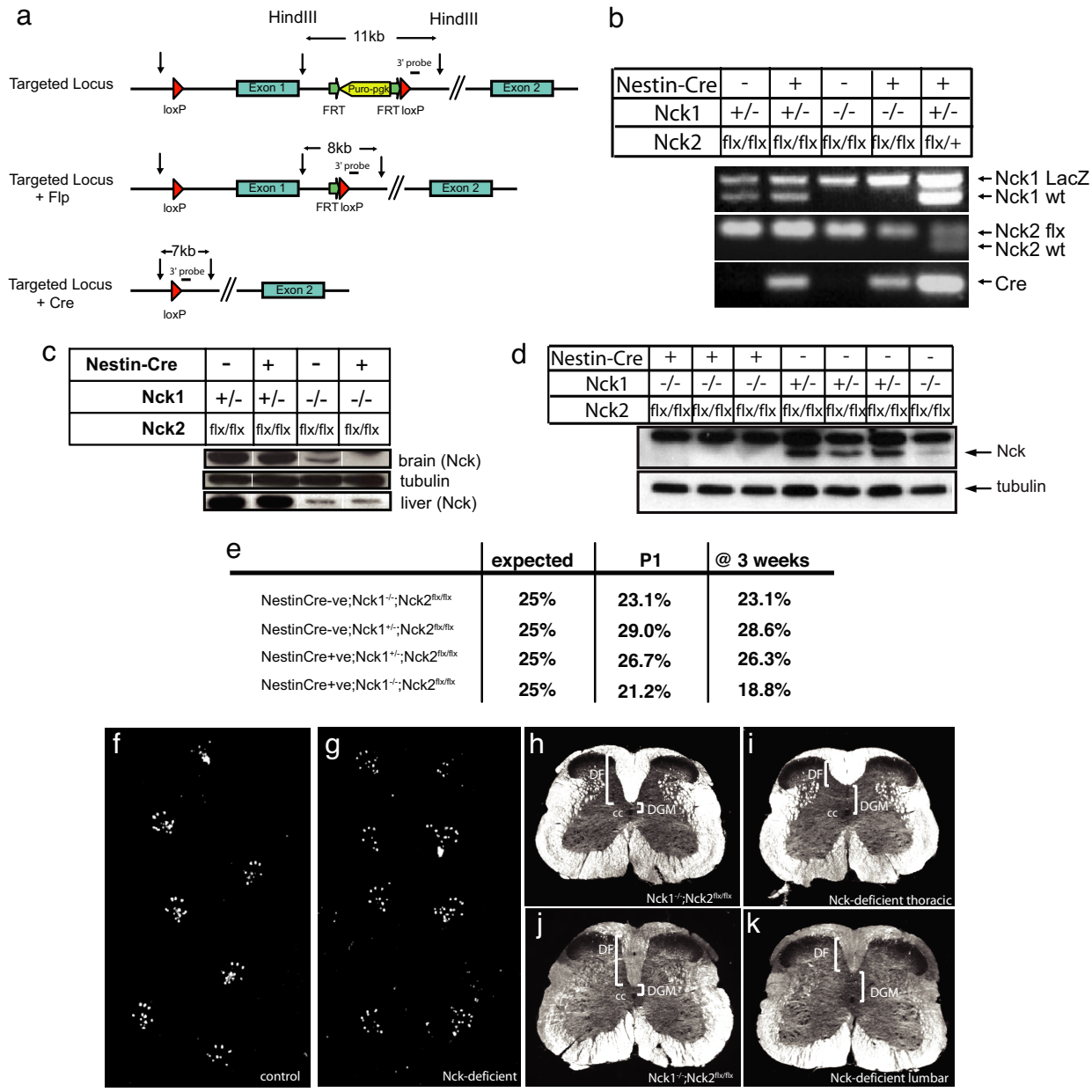

Fig. 1. Generation and characterization of mice containing a conditional allele of *Nck2*. (*a*) Schematic diagram of the strategy used to generate the conditional mutant of Nck2. (*b*) PCR genotyping of mice generated by crossing a *Nck1*$^{-/-}$;*Nck2*$^{flx/flx}$ female with a *Nck1*$^{+/-}$;*Nck2*$^{flx/flx}$;*Nestin-Cre* male. An *Nck1*$^{+/-}$;*Nck2*$^{flx/wt}$;*Nestin-Cre* animal was included as a control (last lane). Top gel, *Nck1* allele; middle gel, *Nck2* allele; bottom gel, *Cre*. (*c*) Proteins isolated from the brain (top gel) or liver (bottom gel) of individual P1 mice, as noted, were immunoblotted with a pan-Nck antibody. (*d*) Dissociated cortical neurons from embryonic day-16 animals of various genotypes, as noted, were immunoblotted with a pan-Nck antibody (lower band, upper gel) and reprobed with tubulin (lower gel). Note the loss of Nck expression with decreasing Nck alleles [lanes 1–3 (0 alleles) < lane 7 (2 alleles) < lanes 4–6 (3 alleles)]. (*e*) Mendelian ratio of the offspring generated from crossing *Nck1*$^{-/-}$;*Nck2*$^{flx/flx}$ females with *Nck1*$^{+/-}$;*Nck2*$^{flx/flx}$;*Nestin-Cre* males ($n > 100$ animals at each time point). (*f* and *g*) Hindpaw prints from a 12-week-old control mouse (*Nck1*$^{-/-}$;*Nck2*$^{flx/flx}$) (*f*) or a Nck-deficient mouse (*Nck1*$^{-/-}$;*Nck2*$^{flx/flx}$;*Nestin-Cre*) (*g*). (*h–k*) Dark-field photographs of spinal cord cross-sections at the thoracic (*h* and *i*) and lumbar (*j* and *k*) level of a control (*Nck1*$^{-/-}$;*Nck2*$^{flx/flx}$) (*h* and *j*) and Nck-deficient (*i* and *k*) mouse. cc, central canal; DGM, dorsal gray matter.

ments by unilaterally injecting biotinylated dextran amine (BDA) into layer-V neurons in the motor cortex of 8- to 12-week-old animals (Fig. 2*a*) and then examined the projections of these axons along the rostral–caudal axis (Fig. 2 *b–e*). In both control (*Nck1*$^{-/-}$;*Nck2*$^{flx/flx}$) and Nck-deficient mice, the CST axons were present through the internal capsule and pons (data not shown). At the spinomedullary junction, almost all of the BDA-labeled axons decussated and projected dorsally as they crossed the midline (Fig. 2 *b* and *c*) to extend down the dorsal column of the spinal cord. A few labeled axons projected ipsilaterally in both control (as reported in ref. 15) and Nck-deficient mice. In control mice, axon innervation in the gray matter of the spinal cord was confined to the contralateral side, with few axons crossing the midline (Fig. 2*d*). However, Nck-deficient animals showed a number of axons that aberrantly recrossed the midline in the gray matter [Fig. 2 *e* (arrows) and *f*]; as well, a few fibers were seen crossing in the white matter [Fig. 2 *e* (arrowhead) and *f*]. These results demonstrate that Nck adaptors are important for the guided projections of mammalian CST axons.

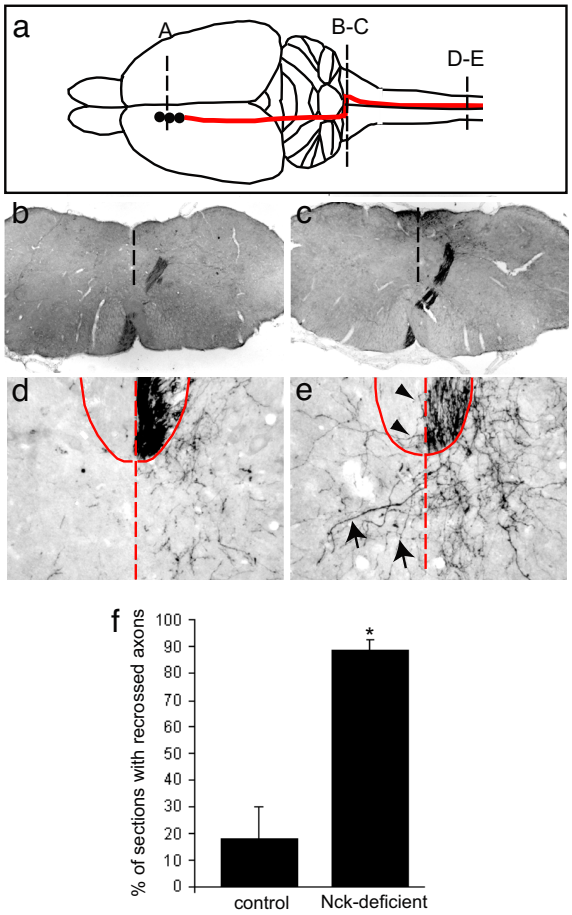

Fig. 2. Reduction of Nck in the developing CNS leads to aberrant axon migration of corticospinal tract fibers. (*a*) Schematic diagram depicting sites of tracer injection in the somatomotor cortex (A) and path of the CST axons from the cortex across the medullary decussation (B-C) into the spinal cord (D-E). (*b* and *c*) BDA-labeled axons are found at the spinomedullary junction (*b*), CST axons decussate in the pyramidal decussation (*c*). (*d* and *e*) Unilateral labeling of CST-positive fibers in the ventral aspect of the DF in both control ($Nck1^{-/-};Nck2^{flx/flx}$) (*d*) and Nck-deficient (*e*) animals at the thoracic level. (*e*) In the Nck-deficient mice, a number of fibers are seen to recross the midline in the gray matter (arrows); in addition, a few fibers were seen crossing in the white matter (arrowheads). The dashed line denotes the spinal midline, and the solid line denotes DF. (*f*) Quantification of recrossing fibers in control ($Nck1^{-/-};Nck2^{flx/flx}$) and Nck-deficient mice ($n = 3$ for each genotype; 70–120 slices per animal). Error bars indicate SD; *, $P < 0.01$ compared with control (Student's *t* test).

Nck-Deficient Mice Exhibit Altered Central Pattern Generator (CPG) Responses and Aberrant Midline Crossing of Spinal Interneuron Projections. CST axons normally innervate commissural interneurons and motor neurons in the lumbar spinal cord during the first and second postnatal week of development (16). However, we observed the hopping phenotype in Nck-deficient animals as early as postnatal day two (P2) (see SI Movie 1 of P4 animals), at which stage the CST axons have not yet innervated their targets. This observation raised the possibility that Nck adaptors also influence axonal projections within the spinal cord segments that control the rhythmic pattern of flexor and extensor muscles, known as the CPG. To pursue this point, we examined the activity of the CPG response in isolated spinal cords from P2 control (Fig. 3*a*) and Nck-deficient (Fig. 3*b*) animals. As shown previously, adding serotonin and NMDA to the control P2 spinal cord produced alternating left–right rhythmic motor activity in ventral roots at both the lumbar (L) 2 (data not shown, $n = 3$) and L5 regions ($n = 6$) (Fig. 3 *a* and *c*). The mean phase for each recording is shown in the circular phase plot (Fig. 3*c*), where 0 represents synchrony between bilateral roots, and 0.5 indicates asynchrony. In contrast, in stimulated spinal cords from Nck-deficient animals, the left and right ventral roots at the L5 ($n = 8$) (Fig. 3 *b* and *d*), L2, and L3 ($n = 5$, data not shown) segmental regions fired simultaneously, indicating a loss of asynchronous behavior.

Left–right coordination is mediated through commissural interneurons (CINs) located in the ventral spinal cord (17, 18). Interneurons positive for the receptor tyrosine kinase EphA4 define a subclass of excitatory rhythmically active neurons that project ipsilaterally and likely innervate motorneurons (19). Both *EphA4*- and *ephrin-B3*-null mice have a hopping phenotype and display synchronous firing of pairs of bilateral ventral motor roots, potentially because of the ectopic projection of excitatory ipsilateral spinal interneurons across the midline (20). To test whether Nck-deficient mice show similar defects, we traced L2 descending CINs by using rhodamine-conjugated dextran amine (RDA). RDA crystals were placed unilaterally in the ventral funiculus at the L4 level in P2 animals, and the axonal projections of these neurons at the L2 level were examined. In both control (Fig. 3*f*) and Nck-deficient animals (Fig. 3*g*), a number of CIN neurons were labeled because of dye uptake from descending CINs (dashed circles in Fig. 3 *f* and *g*), excluding the possibility that the hopping phenotype is due to a loss of these neurons. However, Nck-deficient mice showed an increase in the number of fibers crossing the midline at the L2 level (Fig. 3*g*, arrows). In the contralateral gray matter of Nck-deficient mice, the average labeling intensity was 77.0 ± 5.4 compared with 28.9 ± 2.0 in controls ($P < 0.001$; $n = 5$ and $n = 8$, respectively). These results suggest that Nck mediates intracellular signaling required to establish the neuronal circuitry that generates synchronous firing of ventral motor roots.

The phenotypic similarities between Nck-deficient and EphA4 mutant animals raise the possibility that Nck participates in EphA4 signaling in the spinal cord, consistent with data indicating that Nck2 overexpression can rescue an EphA4-dependent loss-of-cell-adhesion phenotype in *Xenopus* blastomeres (21). We therefore examined the expression of *Nck* genes in the lumbar spinal cord, where EphA4 is present in rhythmically active excitatory interneurons (19). For this purpose, we used mice homozygous for the *Nck1*-null allele, in which a β-gal reporter is fused in-frame with the N-terminal 23 aa of Nck1 (12). These experiments revealed Nck1 expression throughout the spinal gray matter, including throughout the ventral spinal cord (Fig. 3 *h* and *i*). Because a subpopulation of EphA4-positive neurons has been shown to be rhythmically active, with segmentally appropriate CPG responses, and to form excitatory connections with motoneurons (19), we tested whether any Nck1-positive neurons were also EphA4-positive. For this test, we combined EphA4 *in situ* hybridization with β-gal immunostaining on spinal cord sections from P2 $Nck1^{lacZ/+}$ animals. We noted EphA4-positive neurons in the ventrolateral spinal cord that also express Nck1 (arrows in Fig. 3 *j* and *k*). However, not all EphA4-positive cells are detectably Nck1-positive (arrowhead in Fig. 3 *j* and *k*), and not all Nck1-positive cells are EphA4-positive (asterisks in Fig. 3 *j* and *k*). We also confirmed that EphA4 and Nck coimmunoprecipitate using transfected HEK 293T cells and that EphA4 can induce Nck2 tyrosine phosphorylation (Fig. 3*m*). Loss of Nck did not downregulate EphA4 expression in the brain or spinal cord, nor did it cause any change in the localization of ephrin-B3 in the thoracic region of the spinal cord (SI Fig. 6). These data suggest that Nck may signal, in part, through an EphA4-dependent pathway to control CPG responses.

To pursue the notion that aberrantly crossing neurons increase the excitatory input into the contralateral spinal cord, leading to synchronous firing of ventral motor neurons, we treated Nck-deficient spinal cord preparations (P2) with 100 μM sarcosine,

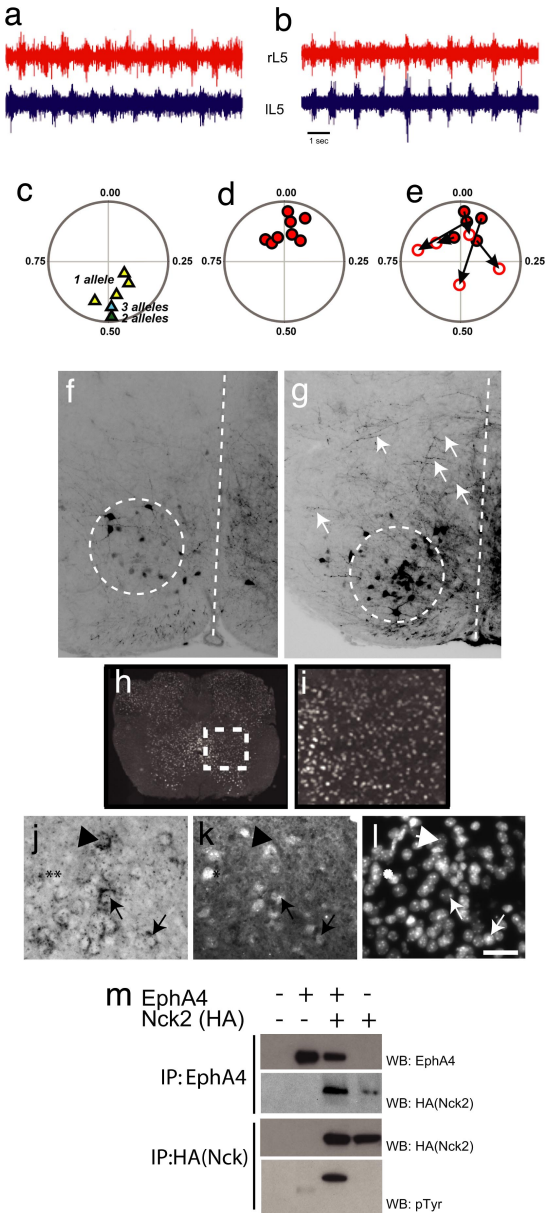

Fig. 3. Loss of Nck leads to synchronous firing in bilateral ventral roots and defects in commissural axon guidance. (*a* and *b*) Representative trace recordings from the left (lL5) and right (rL5) ventral roots at the L5 level after the addition of NMDA and serotonin to isolated spinal cords from P2 control (*Nck1*$^{+/-}$;*Nck2*$^{flx/flx}$;*Nestin-Cre*) (*a*) and an Nck-deficient (*Nck1*$^{-/-}$;*Nck2*$^{flx/flx}$;*Nestin-Cre*) (*b*) mouse. (*c* and *d*) Circular-phase diagrams from control [*Nck1*$^{+/-}$;*Nck2*$^{flx/flx}$;*Nestin-Cre* (yellow triangles; $n = 5$); *Nck1*$^{-/-}$;*Nck2*$^{flx/flx}$ (green triangle; $n = 1$); or *Nck1*$^{+/-}$;*Nck2*$^{flx/flx}$ (blue triangle; $n = 1$)] (*c*) and Nck-deficient [*Nck1*$^{-/-}$;*Nck2*$^{flx/flx}$;*Nestin-Cre* (red circles; $n = 8$)] (*d*) mice. (*e*) Circular-phase diagram of Nck-deficient mice after the addition of 100 μM sarcosine. Filled red circles represent averaged vector plots of individual animals before sarcosine treatment. Open circles identify the final vector plot of individual animals after 20 min of sarcosine treatment. The arrows mark the movement of an individual animal's vector profiles after treatment. All recordings shown are from the L5 level. (*f* and *g*) Epifluorescent images of coronal sections through the L2 spinal cord after contralateral caudal application of rhodamine dextran amine (molecular weight, 3,000) crystals at the L4 level in control *Nck1*$^{-/-}$;*Nck2*$^{flx/flx}$ (*f*) and Nck-deficient (*g*) mice. Descending CINs are found within the dashed circles. Dashed lines mark the midline. Arrows in *g* indicate fibers crossing the midline in Nck-deficient animals. (*h* and *i*) Nck1-β-gal expression of coronal sections through the lumbar spinal cord of an adult mouse. (*i*) Enlargement of boxed region shown in *h*. (*j* and *k*) EphA4-positive cells in the medial–ventrolateral spinal cord (*j*, arrows) that are Nck1-positive (*k*, arrows) as revealed by EphA4 RNA *in situ* hybridization (*j*) and β-gal antibodies (*k*). (*l*) Hoechst staining to show nuclei. (Scale bar: 10 μm.) Not all Nck1-positive cells are EphA4-positive, (*j* and *k*, asterisks), nor are all EphA4- positive cells Nck1-positive (*j* and *k*, arrowheads). (*m*) HEK293T cells were transfected as indicated. Lysates were immunoprecipitated (IP) with antibodies as indicated and probed with anti-EphA4 (top row), anti-HA antibodies (middle two rows), or anti-pTyr antibodies (bottom row).

a glycine uptake inhibitor, and recorded motor neuron activity in L5 roots. In the ephrin-B3 and EphA4 mutants, sarcosine restores asynchronous firing, likely by increasing the inhibitory drive (20). In CPG recordings from Nck-deficient mice, the addition of sarcosine caused a shift in the mean phase value near 0 (V test, 0.03; $P < 0.001$; Fig. 3*d*) to 0.89, ablating any uniform distribution and any statistical sign for a preferred phase value near 0 (Rayleigh's uniformity test, $P > 0.89$; V test, $P = 0.35$; Fig. 3*e*). Thus, sarcosine shifted the left–right firing away from synchrony, but did not fully revert firing to alternation as observed in EphA4 mutants. The incomplete phenotypic rescue by sarcosine may reflect a strong excitatory drive that is too potent to be fully countered by sarcosine-enhanced CIN inhibition. It is also possible that, in addition to EphA4-positive neurons, a population of Nck-positive neurons lacking EphA4 might affect the spinal circuitry, and thus ipsilateral rhythmic pattern generation. Indeed, a subpopulation of the excitatory neurons in the ventro-medial lumbar spinal cord express EphA4 (19), and some EphA4 positive neurons are inhibitory (19, 22).

Nck-Deficient Mice Display Multiple Axon Guidance Defects. Nck-deficient and *EphA4*$^{-/-}$ mice show other differences in addition to their distinct response to sarcosine. Similar to the *EphA4*$^{-/-}$ mice, the DF of the Nck-deficient mice is shallow, but unlike the *EphA4*$^{-/-}$ mice, the DF fails to broaden in the Nck-deficient animals. In this regard, other guidance receptors that bind Nck, including DCC (7, 23), may play a role in the CPG response. We also noted a reduced development of the posterior tract of the anterior commissure (pAC) in Nck-deficient mice (Fig. 4*c*), a phenotype also attributed to defective reverse signaling through the transmembrane ephrins (24). The pAC appeared normal in both the single *Nck1*- (Fig. 4*a*) and *Nck2*-null animals (Fig. 4*b*), suggesting that the Nck proteins can compensate for one another in the pAC. Tyrosine phosphorylated ephrin-B1 has been shown to selectively bind the SH2 domain of Nck2 (5), but it is possible that ephrin-B1 recruits both Nck1 and Nck2 *in vivo*, especially given the markedly similar binding properties of their SH2 domains (25). Furthermore, we have observed a much more severe phenotype, in *Nck1*$^{-/-}$;*Nck2*$^{flx/-}$;*Nestin-Cre* mice, in which one of the *Nck2* alleles is fully null. These animals have a 3-fold reduction in the expression of Nck2 mRNA in the cortex compared with their littermate *Nck1*$^{-/-}$;*Nck2*$^{flx/flx}$;*Nestin-Cre* controls (SI Fig. 5 *c*–*e*). These animals survive the embryonic period and are born at a Mendelian ratio, but most die within a few days of birth, likely because of an inability to suckle because their stomachs are void of milk (J.P.F and T.P., unpublished observations). To date, one such animal survived to P12; this animal was unusually small (SI Fig. 5*f*), severely ataxic, and, in response to stimulation, its hindlimbs went into rhythmic extension/flexion seizure-like activity (see SI Movie 2). These data suggest that the *Nck1*$^{-/-}$;*Nck2*$^{flx/flx}$;*Nestin-Cre* animals described here retain residual Nck function and that the spinal cord defect represents a sensitized phenotype. Nck adaptors may therefore be important in transmitting signals that guide axons downstream of multiple receptors.

Nck Interacts with Actin-Regulatory Proteins and α-Chimaerin. To pursue targets of Nck that might regulate axon guidance, we used MS to identify proteins in a mouse brain lysate that interact with the Nck1 SH3 domains. A number of peptides for previously identified Nck SH3-binding proteins, including synaptojanin, a

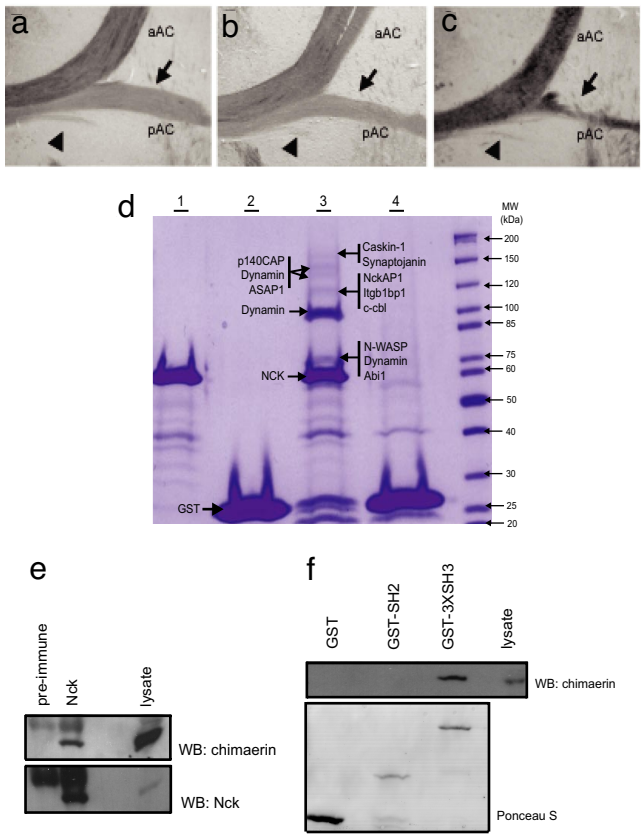

Fig. 4. Nck proteins have multiple functions and interactions in the nervous system. (*a–c*) Loss of Nck leads to defective development of the posterior tract of the anterior commissure. Shown are bright-field images of horizontal sections through the anterior commissure (AC) of 12-week-old animals. Anterior is up. Anterior (aAC), posterior (pAC, indicated by arrows), and a third smaller tract ventral to the pAC fibers (arrowheads) are indicated. (*d*) Colloidal Coomassie stained gel after GST fusion pull-downs as outlined. Lane 1, GST-Nck1-SH3 alone; lane 2, GST alone; lane 3, GST-Nck1-SH3 GST and mouse brain lysate; lane 4, GST and mouse brain lysate. Proteins identified by liquid chromatography tandem MS (LC-MS/MS) are shown beside each arrow. (*e*) Rat brain lysate was immunoprecipitated as indicated. Proteins were detected by immunoblotting with α-chimaerin antibodies (*Upper*) or Nck antibodies (*Lower*). (*f*) Brain lysate was mixed with GST or recombinant GST fusion proteins as indicated. (*Upper*) The immunoblot was probed for α-chimaerin. (*Lower*) Ponceau S stain of blot to show level of fusion protein.

phosphoinositide phosphatase, NckAP1, c-cbl, dynamin, Abi1 and N-WASP were detected (Fig. 4*d* and SI Table 1). In addition, 16 peptides were identified for p140Cap, which regulates actin dynamics downstream of adhesion molecules (26). These data support the contention that the SH3 domains of Nck link to actin regulatory proteins in the nervous system, including N-WASP and WAVE complex members. Previously, we have shown that the Rac GTPase activating protein (GAP) protein α-chimaerin can interact with Nck (27). We find that endogenous Nck precipitates α-chimaerin (among other proteins) from brain lysate (Fig. 4*e*) and that the SH3 domains of Nck are responsible for this interaction (Fig. 4*f Upper*). In this regard, mice deficient in α-chimaerin have a hopping phenotype similar to Nck-deficient animals and *EphA4*$^{-/-}$ mice and display defects in the midline repulsion of CST and ipsilateral spinal interneurons similar to Nck-deficient mice (28–30). Taken together, the biochemical and phenotypic data suggest that EphA4, Nck, and α-chimaerin function in a related pathway to control axon guidance, consistent with recent evidence from α-chimaerin mutant mice (28–30).

These data establish that mammalian Nck SH2/SH3 adaptors convey signals to control the projections of spinal cord neurons that direct limb movement. Nck is also necessary for the development of specialized actin-based structures (foot processes) in kidney podocytes (1) that form an essential part of the filtration barrier; together, these results indicate that Nck functions in different cell types to couple distinct receptors to the cytoskeleton and thereby cooperates in fashioning specialized cellular morphologies. In spinal cord neurons, Nck likely promotes growth cone retraction, as indicated by the aberrant projections of Nck-deficient excitatory neurons across the midline, whereas in the kidney Nck promotes the outgrowth and stabilization of foot processes (1). Neurons and podocytes may respond differently to common Nck targets, such as the Arp2/3 complex (downstream of N-WASP) and Pak, which in many cell types are involved in cellular protrusions (31). Interestingly, defects in signaling from Pak and the N-WASP-Arp2/3 complex suppress the responses of cultured neuronal cells to repellant guidance cues (32–34). It is also possible that different cells express distinct repertoires of targets for the Nck SH3 domains and associate with different affinities and kinetics with tyrosine-phosphorylated receptors. In summary, we identify Nck as a cytoplasmic regulator of mammalian axon guidance cues *in vivo* and indicate that adaptor proteins can contribute to the organization of complex neuronal circuitry.

Methods

Generation of Mice. *Nck1* and *Nck2* mutant mice have been described in ref. 12. For the generation of the floxed targeting vector, genomic fragments were isolated from a 129/SV-Ola library. The Nck2 vector contained a 9.5-kb genomic fragment, including the first coding exon (7.75 kb 5′ arm, 1.75 kb 3′ arm). LoxP sites were inserted 500 bp 5′ and 5.5 kb 3′ of the first coding exon. The Puro-pgk cassette flanked by Flip recombination sites was inserted immediately upstream of the 3′ loxP site. Embryonic stem (R14-ES) cells were electroporated; positive ES clones were injected into ICR blastocysts to generate heterozygous mutant mice. These mice were then crossed onto an *Nck2*-null mouse to generate *Nck2*$^{flx/-}$ mice. The Puro-pgk cassette was removed by injecting fertilized eggs from *Nck2*$^{flx/-}$ mice with a vector containing Flip recombinase, injected eggs were returned to pseudopregnant females, and resulting offspring were screened for excision of the Puro-pgk cassette. These animals were then crossed onto the *Nck1*-null background and then were crossed with a *Nestin-Cre* transgenic mouse (a kind gift from R. Klein, European Molecular Biology Laboratory, Heidelberg).

PCR Screening of Gene-Targeted Mouse Strains. Template DNA for genomic PCR was isolated from ear tissue or tail tissue as described in ref. 12. Cre-positive animals were identified using the following primers: forward, 5′-GTTATAAGCAATCCCCAGAAATG; reverse, 5′-GGCAGTAAAAACTATCCAGACA. For the floxed *Nck2* animals, the following primers were used: forward, 5′-GGATACCACATTGGCATTAGTAG; reverse, 5′-GTGCTCATTTGACAAGTGACAC. Genotyping for the *Nck1* and *Nck2* alleles have been described in ref. 12. For the quantitative RT-PCR, the following primers were used: 5′-AGGACAGGCTACGTGCCTT; reverse, 5′-GTACTCCGCATCAGTGCTTGG by using the 2(Delta Delta C(T)) method (35).

Surgery and Staining. For anterograde tracing, anesthetized adult mice ($n = 5$, *Nck1*$^{-/-}$;*Nck2*$^{flx/flx}$;*Nestin-Cre*; $n = 3$, *Nck1*$^{-/-}$;*Nck2*$^{flx/flx}$) were unilaterally injected at three sites as described in ref. 15. In total, 0.4 μl per site of a solution containing 10% biotinylated dextran amine (BDA) in 0.1 M phosphate buffer (PB) (Molecular Probes) was injected into each position in the sensorimotor area. After a survival time of 14–30 days, the animals were killed with an overdose of Somnitol, the BDA signal was enhanced using the Vectastain ABC Elite Kit, and diaminobenzidine (DAB) reagent was used to detect the signal.

Spinal Cord Tracing. To identify commissural neurons, we performed labeling experiments as described in ref. 20. Microscopy was carried out using a Leica DMRX microscope equipped with fluorescence and transmitted light optics. ImageJ (National Institutes of Health, http://rsb.info.nih.gov/ij) was used to define and analyze intensity (average pixel intensity of 8-bit range) in a square region of interest approximately one-sixth the size of a hemicord (in the gray matter adjacent to the midline). Images were inverted in Adobe Photoshop to define fibers.

Recording Ventral Root Activity. Each spinal cord isolated from 2-day-old mice was transferred to a recording chamber perfused with oxygenated saline maintained at 25°C. Right–left pairs of lumbar roots (L2–L5) were drawn into separate suction electrodes each containing a silver wire (chloride-coated) recording electrode connected to headstages of a MultiClamp 700A dual channel amplifier (Axon Instruments/Molecular Devices). Responses were amplified, bandpass-filtered (0.1–2 kHz), digitized, and stored onto a computer by using pCLAMP9 software. Rhythmic motor output was induced by application of 5 μM NMDA/serotonin, and in some experiments sarcosine (100–200 μM) was also added.

Quantification of Rhythmic Discharges. After ventral root recordings were rectified and smoothed with low-pass filtering (0.2 s), we performed a semi-automated analysis to find burst-discharge peak times by using the Event Detection feature of Clampfit version 9.2 (Axon Instruments/Molecular Devices). Oriana software was used to statistically determine whether the grouped phases were uniformly distributed (Rayleigh's test, $P < 0.05$) or whether the phase distribution had a specified mean direction (*V* test).

ACKNOWLEDGMENTS. We thank Dr. Patrick Whelan (University of Alberta, Alberta, Canada) for his help and guidance; Dr. Ole Kiehn (Karolinska Institute, Stockholm) for his helpful advice in establishing the electrophysiological studies; Dr. Phillipe Monnier and Franco Taverna (both at the University of Toronto) for analysis of the animals; Ken Harpel (University of Toronto) for the histological sections used in this study; Kelly Elder for technical assistance; Dr. Mark Henkemeyer (University of Texas Southwestern, Dallas) for the kind gift of the ephrin-B3 knockout mice; Drs. Robert Brownstone and Mark Nachtigal (Dalhousie University) for technical advice and suggestions on the manuscript; and Dr. Andrea Betz (Max Planck Institut, Göttingen, Germany) for the α-chimaerin antibodies and for sharing data before publication. This work was supported by grants from the Canadian Institutes for Health Research (to T.P., J.C.R., and J.P.F.) and the National Cancer Institute of Canada (to T.P.). B.J.S. holds a Canadian Institutes for Health Research doctoral award. J.P.F. holds a Tier 2 Canadian Research Chair in Brain Repair, and J.C.R. holds a Tier1 Canadian Research Chair in Learning and Memory. T.P. is a Distinguished Scientist of the Canadian Institutes for Health Research.

1. Jones N, Blasutig IM, Eremina V, Ruston JM, Bladt F, Li H, Huang H, Larose L, Li SS, Takano T, *et al.* (2006) *Nature* 440:818–823.
2. Li W, Fan J, Woodley DT (2001) *Oncogene* 20:6403–6417.
3. Holland SJ, Gale NW, Gish GD, Roth RA, Songyang Z, Cantley LC, Henkemeyer M, Yancopoulos GD, Pawson T (1997) *EMBO J* 16:3877–3888.
4. Stein E, Huynh-Do U, Lane AA, Cerretti DP, Daniel TO (1998) *J Biol Chem* 273:1303–1308.
5. Cowan CA, Henkemeyer M (2001) *Nature* 413:174–179.
6. Fan X, Labrador JP, Hing H, Bashaw GJ (2003) *Neuron* 40:113–127.
7. Li X, Meriane M, Triki I, Shekarabi M, Kennedy TE, Larose L, Lamarche-Vane N (2002) *J Biol Chem* 277:37788–37797.
8. Pramatarova A, Ochalski PG, Chen K, Gropman A, Myers S, Min KT, Howell BW (2003) *Mol Cell Biol* 23:7210–7221.
9. Morimoto C, Tachibana K (1996) *Hum Cell* 9:163–168.
10. Garrity PA, Rao Y, Salecker I, McGlade J, Pawson T, Zipursky SL (1996) *Cell* 85:639–650.
11. Hing H, Xiao J, Harden N, Lim L, Zipursky SL (1999) *Cell* 97:853–863.
12. Bladt F, Aippersbach E, Gelkop S, Strasser GA, Nash P, Tafuri A, Gertler FB, Pawson T (2003) *Mol Cell Biol* 23:4586–4597.
13. Tronche F, Kellendonk C, Kretz O, Gass P, Anlag K, Orban PC, Bock R, Klein R, Schutz G (1999) *Nat Genet* 23:99–103.
14. Christensen LO, Petersen N, Morita H, Nielsen J (1998) *Ann NY Acad Sci* 860:546–549.
15. Steward O, Zheng B, Ho C, Anderson K, Tessier-Lavigne M (2004) *J Comp Neurol* 472:463–477.
16. Gianino S, Stein SA, Li H, Lu X, Biesiada E, Ulas J, Xu XM (1999) *Brain Res Dev Brain Res* 112:189–204.
17. Kiehn O, Butt SJ (2003) *Prog Neurobiol* 70:347–361.
18. Butt SJ, Lebret JM, Kiehn O (2002) *Brain Res Brain Res Rev* 40:107–117.
19. Butt SJ, Lundfald L, Kiehn O (2005) *Proc Natl Acad Sci USA* 102:14098–14103.
20. Kullander K, Butt SJ, Lebret JM, Lundfald L, Restrepo CE, Rydstrom A, Klein R, Kiehn O (2003) *Science* 299:1889–1892.
21. Bisson N, Poitras L, Mikryukov A, Tremblay M, Moss T (2007) *Mol Biol Cell* 18:1030–1043.
22. Lundfald L, Restrepo CE, Butt SJ, Peng C, Droho S, Endo T, Zeilhofer HU, Sharma K, Kiehn O (2007) *Eur J Neurosci* 26:2989–3002.
23. Finger JH, Bronson RT, Harris B, Johnson K, Przyborski SA, Ackerman SL (2002) *J Neurosci* 22:10346–10356.
24. Cowan CA, Yokoyama N, Saxena A, Chumley MJ, Silvany RE, Baker LA, Srivastava D, Henkemeyer M (2004) *Dev Biol* 271:263–271.
25. Frese S, Schubert WD, Findeis AC, Marquardt T, Roske YS, Stradal TE, Heinz DW (2006) *J Biol Chem* 281:18236–18245.
26. Di Stefano P, Cabodi S, Boeri Erba E, Margaria V, Bergatto E, Giuffrida MG, Silengo L, Tarone G, Turco E, Defilippi P (2004) *Mol Biol Cell* 15:787–800.
27. Wells CD, Fawcett JP, Traweger A, Yamanaka Y, Goudreault M, Elder K, Kulkarni S, Gish G, Virag C, Lim C, *et al.* (2006) *Cell* 125:535–548.
28. Beg AA, Sommer JE, Martin JH, Scheiffele P (2007) *Neuron* 55:768–778.
29. Wegmeyer H, Egea J, Rabe N, Gezelius H, Filosa A, Enjin A, Varoqueaux F, Deininger K, Schnutgen F, Brose N, *et al.* (2007) *Neuron* 55:756–767.
30. Iwasato T, Katoh H, Nishimaru H, Ishikawa Y, Inoue H, Saito YM, Ando R, Iwama M, Takahashi R, Negishi M, *et al.* (2007) *Cell* 130:742–753.
31. McCarty JH (1998) *BioEssays* 20:913–921.
32. Marler KJ, Kozma R, Ahmed S, Dong JM, Hall C, Lim L (2005) *Mol Cell Biol* 25:5226–5241.
33. Strasser GA, Rahim NA, VanderWaal KE, Gertler FB, Lanier LM (2004) *Neuron* 43:81–94.
34. Guan S, Chen M, Woodley D, Li W (2007) *Mol Cell Biol.*
35. Livak KJ, Schmittgen TD (2001) *Methods* 25:402–408.